Control Neuro-Fuzzy of a Dual Star Induction Machine (DSIM) supplied by Five-Level Inverter

Larafi Bentouhami[a,b], Rachid Abdessemed[b], Abdelhalim Kessal[a,*], Elkhier Merabet[a,b]

[a]Faculty of Sciences & Technology, Bordj Bou Arreridj University, Algeria
[b]LEB-Research Laboratory, Department of Electrical Engineering, University of Mostapha ben Boulaid, Batna-2, Algeria

Abstract

This work relates to a hybrid scheme (Neuro-Fuzzy) for speed control of a dual star induction motor (DSIM) with enhanced performance. A 4-layer network is utilized to set the Fuzzy elements in order to minimize error square. To control this machine, two five-level inverters with PWM techniques are introduced and an indirect field oriented method is used. Simulation results are presented for the NF controller; it is observed that the NFC gives better responses and robustness for the speed control of this machine with its load disturbances and parameter variations, such as increased rotor resistance and moment of inertia. The results are compared with results obtained from a conventional inverter. Notably, there is a great drop in the stator currents, and the magnitude of the pulsating electromagnetic torque is reduced for a five-level inverter compared with a conventional inverter.

Keywords: Dual star induction machine (DSIM), Indirect field oriented control (IFOC), five-level inverter, Neuro-fuzzy cntroller (NFC)

1. Introduction

Poly-phase machines exist to cover multiple tasks and special profits (such as reduced couple pulsations, mitigate total harmonic distortion, high power/current ratio) can be invested to justify the great complexity with regard to three-phase case [1–4].
Emil Levi [5] summarizes new developments in the field of control of poly-phase induction machine control. Conventional proportional-integral (PI), proportional-integral-derivative (PID) controllers are employed in speed and current controllers, but the designs of these controllers depend on the exact machine model with accurate parameters, and are very sensitive to machine parameter variations, load disturbances and rotor resistance variations [6–8]. Mathematical modeling is not needed for the development of advanced controllers. Numerous methods have been proposed to replace conventional proportional-integral (PI), proportional-integral-derivative (PID) controllers, such as the fuzzy logic controller (FLC) [9–11] and artificial neural networks (ANNs) [12–14]. To improve fuzzy controller performance, manual tweaking is needed [7] and it is important to train the neural controller for all operating cases [15]. The

Neuro-Fuzzy Controller (NFC) controls the induction motor drive and has the advantages of both the FLC and ANN. So, in this paper, an NFC for speed control of a DSIM drive system is proposed. The NFC developed in the early 90s by Jang [16–18] combines the concepts of fuzzy logic and neural networks to form a hybrid intelligent system that enhances the ability to automatically learn and adapt. An ANN is used to adjust input and output parameters of membership functions in the FLC. The back propagation learning algorithm is used to train this network.

In recent years multi-level inverters have become very popular for industrial and power system applications, due to their advantages over conventional inverters, i.e., High Power rating, Low Harmonics. Some studies about modeling and analysis of the dual star induction machine supplied by multi-level inverters were done individually [19–21], but there has been no study into control of this machine fed by multi-level inverters. So, in this study an advanced control scheme using neuro-fuzzy (NF) is proposed to control a dual star induction machine (DSIM) supplied by two 5–level voltage sources (PWM) inverters used in association with indirect field oriented control. A comparison with the results of the conventional inverter is given.

The simulated model results show very convincing performances with introduced load disturbances and parameter variations, such as increased rotor resistance and moment

---
*Corresponding author
Email address:* `abdelhalim.kessal@yahoo.fr` (Abdelhalim Kessal)
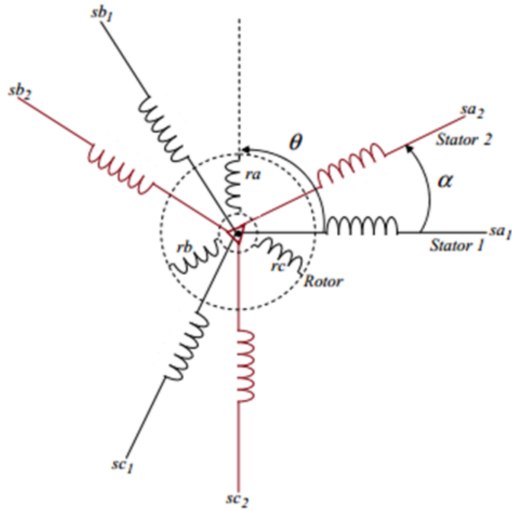
Figure 1: Schematic diagram of the dual star induction machine

of inertia. A detailed Matlab model for indirect field oriented control of DSIM fed by two voltage source inverters integrating the proposed NFC is developed.

The paper is organized as follows: in Sections 2 and 3, the DSIM and IFOC are explained; Section 4 presents the model and control of a five-level inverter; the design of the NFC controller are shown in Section 5; Section 6 contains the simulation results. Finally, the conclusions are in Section 7.

2. Machine model

A common type of multiphase machine is the dual star induction machine (DSIM), where two sets of three-phase windings, spatially phase shifted by 30 electrical degrees, share a common stator magnetic core, as shown in Fig. 1 [9]. Modeling and control of DSIM in the original reference frame would be very difficult. For this reason, a simplified model is required. As a consequence, the mathematical modeling approach of DSIM is similar to the standard induction machine ones and usually it is obtained using the same simplifying assumptions as cited in [9].

In the induction machines, rotor winding has a short-circuit hence v_{dr}=0 and v_{qr}=0.

The mechanical equations are given by equations (1) and (2):

$$T_{em} = P \frac{L_m}{L_m + L_r} \left[\phi_{dr}(i_{qs1} + i_{qs2}) - \phi_{qr}(i_{ds1} + i_{ds2}) \right] \quad (1)$$

$$\frac{J}{P} \frac{d}{dt} \omega_r = T_{em} - T_L - \frac{K_f}{P} \omega_r \quad (2)$$

where: ω_s , ω_r—speed of synchronous reference frame and electrical rotor speed, l_s , l_r—stator and rotor inductances, L_m- resultant magnetizing inductance, P—number of pole pairs, J—moment of inertia, T_L—load torque, K_f—total viscous friction coefficient.

3. Indirect Field Oriented Control of a DSIM

The main goal of field-oriented control (FOC) is to obtain decoupled control of electromagnetic torque and rotor flux of the motor as in DC machines [9]. Due to its simplicity and low cost, the ideal field oriented control method is commonly used. The d-axis is aligned with the rotor flux space vector. In IFOC the rotor flux linkage axis is forced to align with the d-axis, and it follows that the direct flux equals the reference, equation (3):

$$\phi_{dr} = \phi_r^* \quad (3)$$

The quadratic component of the flux, as (4):

$$p\phi_{dr} = \phi_{qr} = 0 \quad (4)$$

The slip speed ω_{sl} and component references of stator current can be expressed by equations ((5),(6) and (7)):

$$\omega_{sl}^* = \frac{R_r L_m}{(L_m + l_r)\phi_r^*} i_{qs}^* \quad (5)$$

$$i_{ds}^* = \frac{1}{L_m} \phi_s^* \quad (6)$$

$$i_{qs}^* = \frac{(Lm + Lr)}{PL_m \phi_r^*} T_{em}^* \quad (7)$$

where:

$$i_{ds}^* = i_{ds1}^* + i_{ds2}^* \quad (8)$$

$$i_{qs}^* = i_{qs1}^* + i_{qs2}^* \quad (9)$$

$$Tr = \frac{l_r}{R_r} \quad (10)$$

q-axes currents are re-labeled as flux-producing (i_{qs}^*) and torque-producing (i_{qs}^*) components of the stator current phases, respectively.

T_r: denotes the rotor time constant.

To generate two sets of command/reference voltage vectors $(v_{ds1}^*, v_{qs1}^*, v_{ds2}^*$ and $v_{qs2}^*)$, two independent pairs of PI controllers are introduced.

4. Model and control of a five-level inverter

Current research focuses on various kinds of multilevel inverters [22–24]. In this work, a 5-level three-phase cascaded hybrid multilevel inverter includes a standard 3-leg inverter and H-bridge in series with each inverter leg given in Fig.2 [25]. A PWM signal modulated technique (triangular sinusoidal) is used to govern the multilevel converter.

Fig. 3 shows single phase 5-level inverter output, 4 carriers with the same frequency and amplitude.
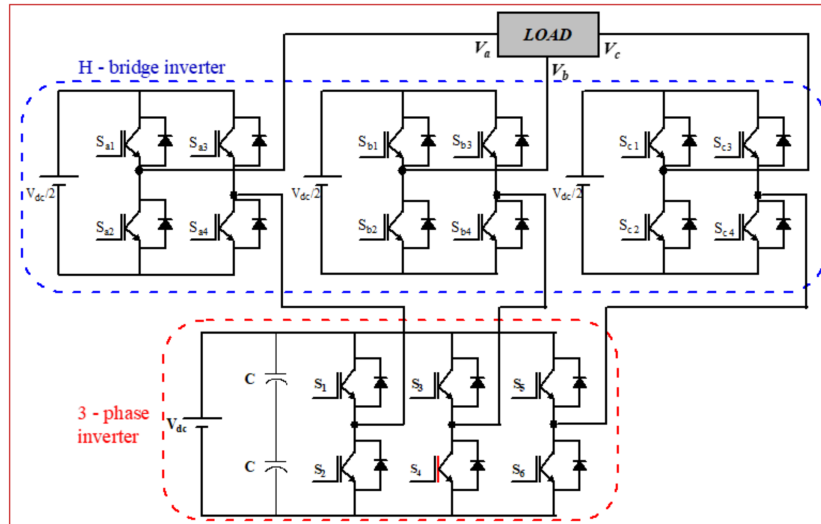
Figure 2: Five-level three-phase cascaded hybrid multilevel inverter structure
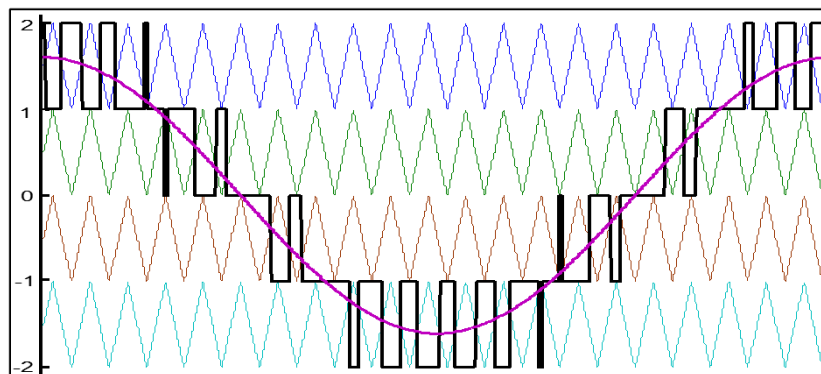

Figure 3: Single phase five-level inverter output
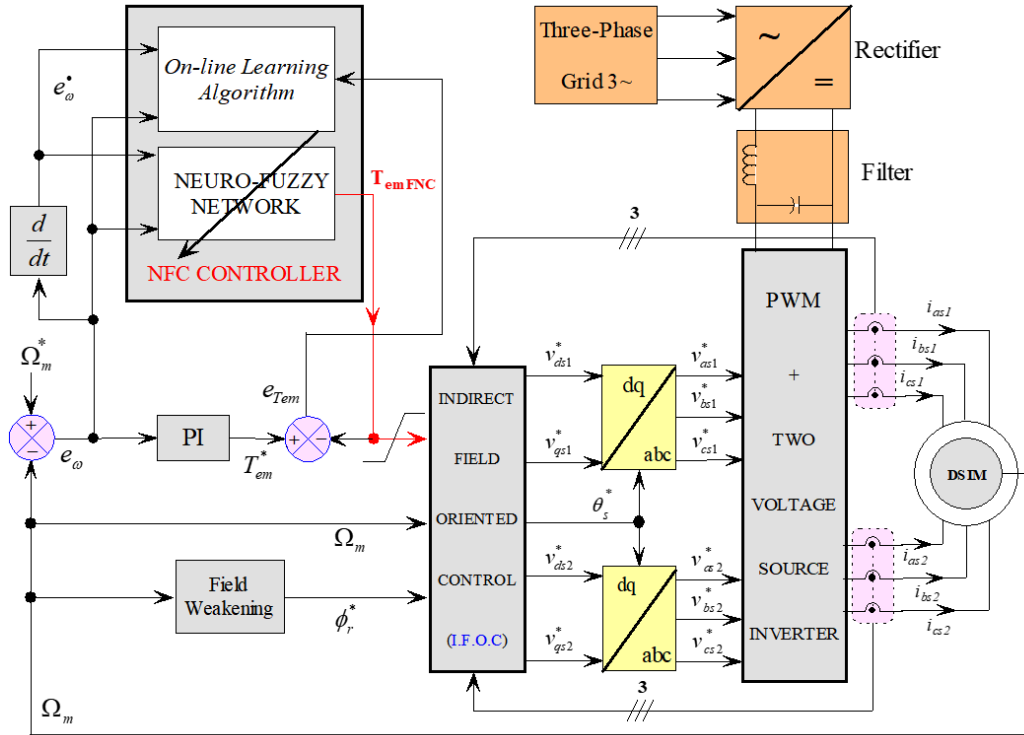
Figure 4: Block diagram NFC with IFOC of regulation speed of DSIM

5. Design of the NFC Controller

The NFC is composed of an on-line learning algorithm with a neuro-fuzzy network (see scheme in Fig. 4). The neuro-fuzzy network is trained using an on-line learning algorithm. The speed error e_ω and error-changing $_\omega$ are the inputs of the proposed NFC, whilst torque command T_{emNFC} is the output of the proposed neuro-fuzzy controller [26, 27]. In Fig. 5, 4 layers are given: the first is for inputs, the second for fuzzification, the next represents rule evaluation and the last layer for defuzzification.

The goal of the PI controller is to obtain the desired electromagnetic torque T_{em}^*, e_{Tem} represents the error between the desired torque T_{em}^* and the control torque T_{emNFC}^* (its current value given by NFC).

Detailed discussions on the various layers of the neuro-fuzzy network are given below.

Input Layer: Each input node in this layer corresponds to the specific input variable, the inputs of this layer are given by $net_1^I = e_\omega$ and $net_2^I = \dot{e}_\omega$.

The outputs of this layer are given by:

$y_1^I = f_1^I(net_1^I) = e_\omega$ and $y_2^I = f_2^I(net_2^I) = \dot{e}_\omega$

The weights of this layer are unity and fixed.

Fuzzification Layer: Each node performs a membership function that can be referred to as the fuzzification procedure; seven (7) memberships based on the Gaussian function are applied, as shown in Fig. (6), and defined by (11) and (12):

$$net_{i,j}^{II} = -\left(\frac{x_{i,j}^{II} - m_{i,j}^{II}}{\sigma_{i,j}^{II}}\right)^2 \qquad (11)$$

$$y_{i,j}^{II} = f_{i,j}^{II}\left(net_{i,j}^{II}\right) = \exp\left(net_{i,j}^{II}\right) \qquad (12)$$

where: $m_{i,j}^{II}$ and $\sigma_{i,j}^{II}$, (i=1;2) are the mean and the deviation of the Gaussian function.

Rule Layer: The total number of rule in this layer is 49 (7×7 = 49), each node is a fixed and noted Π, for represent a rule base used in the FLC, a product operator is used in each node. Fig. (7) shows surface plot showing relationship between input and output parameters. The values of weights between Rule layer and Fuzzification layer are unity.

Defuzzification Layer: Output is given by gravity center method; each node equation is given as:

$$a = \sum_j \sum_k (w_{jk}^{IV} y_{jk}^{III}) \;;\; b = \sum_j \sum_k (y_{jk}^{III}) \qquad (13)$$

$$net_0^{IV} = \frac{a}{b} \;;\; y_0^{IV} = f_0^{IV}\left(y_0^{IV}\right) = \frac{a}{b} \qquad (14)$$

w_{jk}^{IV} represents the values of the output membership functions used in the FLC as shown in Fig. (8). y_0^{IV}—is output of the Defuzzification layer. a and b are the numerator and the denominator of the function used in the center of area method, respectively. In the NFC, the goal of learning algorithm is adjustment the weights w_{jk}^{IV}, the m_{1j}^{II}, m_{2k}^{II} and σ_{1j}^{II}, σ_{2k}^{II}. For the learning algorithm we use the supervised gradient descent method. So the error E (equation (15)), we take to describe the back propagation algorithm.
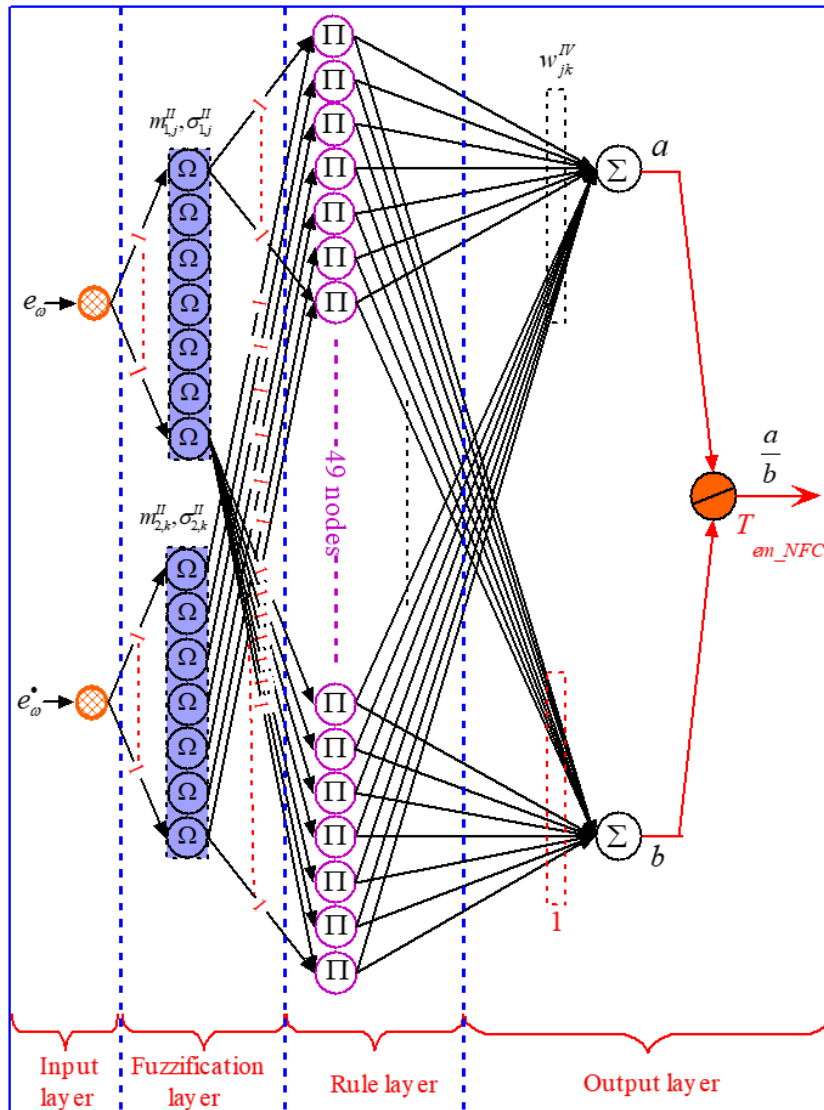
Figure 5: Neuro-fuzzy network structure
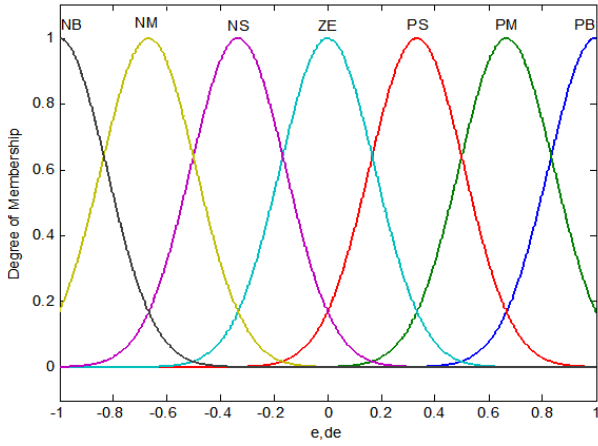
Figure 6: Membership functions for inputs "e" and "de"
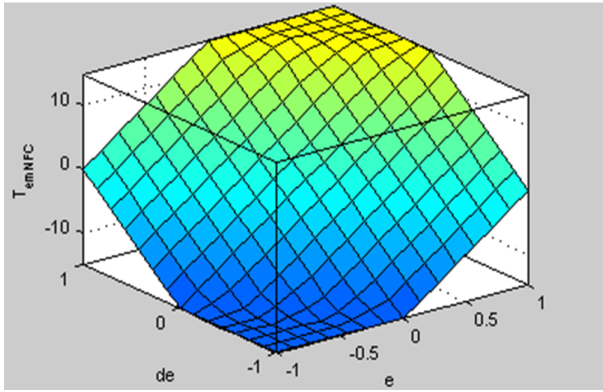
Figure 7: Input / Output surface plot

$$E(l) = \frac{1}{2} e_{Tem}^2 \tag{15}$$

Where the error value can be written as symmetric rules table, equation (16)

$$e_{Tem} = d - y \tag{16}$$

Where, d: is the desired torque control T_{em}^* (Output of PI controller) and y, is the instantaneous output (NFC output "T_{emNFC}").

5.1. The back propagation algorithm

Output layer: The input error is given as:
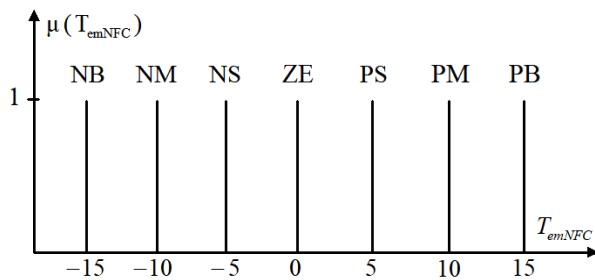
Figure 8: Membership functions for output "T_{emNFC}"

$$\delta_0^{IV} = -\frac{\partial E}{\partial t_0^{IV}} = -\frac{\partial E}{\partial e} \cdot \frac{\partial e}{\partial y} \cdot \frac{\partial y}{\partial t_0^{IV}} = e \tag{17}$$

The variations Δw_{jk}^{IV} of the weights w_{jk}^{IV} to minimize the error can be determined by the generalized delta rule as follows:

$$\Delta w_{jk}^{IV} = -\frac{\partial E}{\partial w_{jk}^{IV}} = \frac{1}{b} \delta_0^{IV} y_{jk}^{III} \tag{18}$$

Finally, the weights w_{jk}^{IV} can be updated to minimize the error as follows:

$$w_{jk}^{IV}(t) = w_{jk}^{IV}(t-1) + \mu_w \Delta w_{jk}^{IV}(t) \tag{19}$$

Where μ_w : is the learning rate for w_{jk}^{IV}.
Rule layer: The error received by this layer from the output layer is computed as:

$$\delta_{jk}^{III} = -\frac{\partial E}{\partial t_{jk}^{III}} = \frac{1}{b} \delta_o^{IV} \left(w_{jk}^{IV} - y \right) \tag{20}$$

Fuzzification layer: The error received from the rule layer is calculated as:

$$\delta_{1,j}^{II} = -\frac{\partial E}{\partial t_{1,j}^{II}} = \sum_k \delta_{jk}^{III} y_{jk}^{III} \tag{21}$$

$$\delta_{2,k}^{II} = -\frac{\partial E}{\partial t_{2,k}^{II}} = \sum_j \delta_{jk}^{III} y_{jk}^{III} \tag{22}$$

In this layer, the changes of m_{1j}^{II}, m_{2j}^{II} and $\sigma_{1j}^{II}, \sigma_{2k}^{II}$ are written as:

$$\Delta m_{i,j}^{II} = -\frac{\partial E}{\partial m_{i,j}^{II}} = \delta_{i,j}^{II} \frac{2 \left(x_{i,j}^{II} - m_{i,j}^{II} \right)}{\left(\partial_{i,j}^{II} \right)^2} \tag{23}$$

$$\Delta \partial_{i,j}^{II} = -\frac{\partial E}{\partial \sigma_{i,j}^{II}} = \delta_{i,j}^{II} \frac{2 \left(x_{i,j}^{II} - m_{i,j}^{II} \right)^2}{\left(\partial_{i,j}^{II} \right)^3} \tag{24}$$

Membership parameters adaptation is obtained through the following:

$$m_{i,j}^{II}(t) = m_{i,j}^{II}(t-1) + \mu_m \Delta m_{i,j}^{II}(t) \tag{25}$$

$$\sigma_{i,j}^{II}(t) = \sigma_{i,j}^{II}(t-1) + \mu_\sigma \Delta \sigma_{i,j}^{II}(t) \tag{26}$$

Where: μ_m, μ_σ: are learning rates, respectively, for $m_{1(2),j(k)}^{II}$ and $\sigma_{1(2),j(k)}^{II}$.

6. Simulation Results and Discussion

The technical parameters are: 2 poles, 4.5kW, 220v / phase, 50 Hz, 2753 rpm. The parameters of the DSIM are reported in the Appendix. In this section, the simulation results obtained in MATLAB software are presented and discussed.

To evaluate the performances of the NFC following the machine parameter variations, various operating conditions are applied, namely load torque and rotor resistance variations, speed reference reversal (2500 rpm, -2500rpm) reference speed with an increased moment of inertia ($\triangle$J % = +50%) on no load. Fig. (9), show the imposed temporary evolution of the load torque and rotor resistance.

It can be seen in Fig. (10)a that the rotor speed follows its reference (2,500 rpm) in a good manner regardless of the
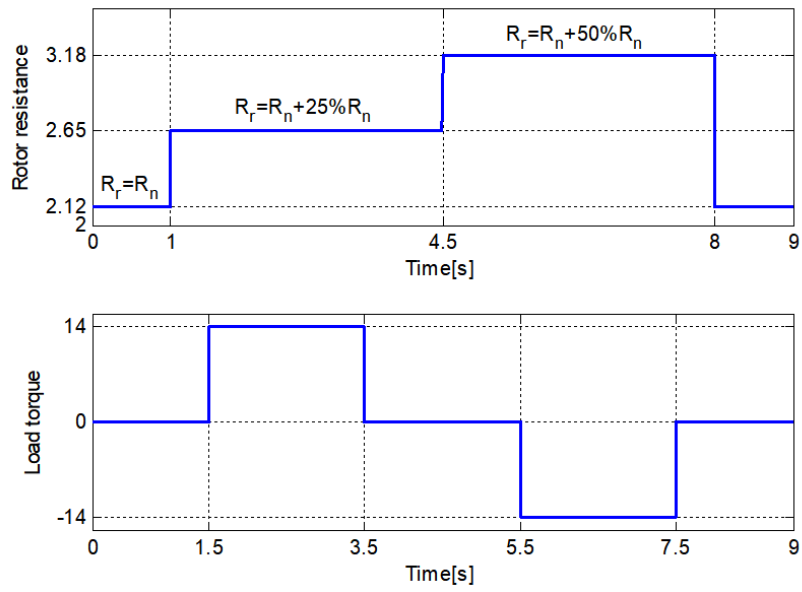
Figure 9: Variation of rotor resistance and load torque.
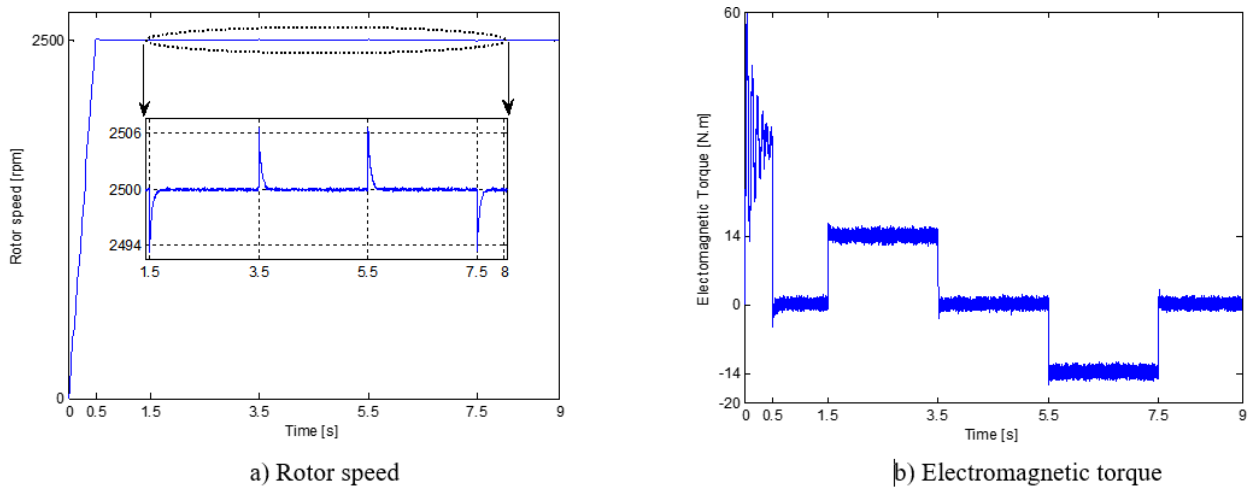
a) Rotor speed

b) Electromagnetic torque
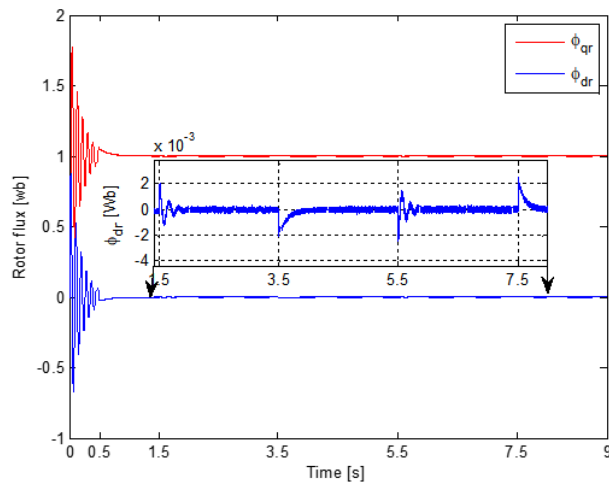
c) d-q axis rotor flux

Figure 10: Simulation results at step reference speed (2500 rpm) under variable (load, rotor resistance) condition

Table 1: Motor Parameters

Parameters	Identifiers & values
Stator resistance, R_s, Ω	3.72
Rotor resistance, R_r, Ω	2.12
Stator leakage inductance, L_s, H	0.022
Rotor leakage inductance, L_r, H	0.006
Resultant magnetizing inductance, L_m, H	0.3672
Moment of inertia, J, $kg \cdot m^2$	0.0662
Viscous friction coefficient, K_f, $kg \cdot m^2/s$	0.001

torque value and the rotor resistance. Fig. (10)b) also shows that the electromagnetic torque follows load torque.

The component of the rotor flux (quadratic and direct) follows its references values, as in Fig. (10)c).

Consequently, the proposed structure is robust from the point of view of variation.

In order to show the influence of the level inverter on the phase current quality and electromagnetic torque ripples, other simulations were conducted when DSIM is fed by two voltage sources: with a conventional inverter and a five-level inverter Fig. (11).

Fig. (11) shows the results obtained when step changes of load torque Tr = 21N.m at t = [1 2]s and speed inversion were applied at t = 2.5s to evaluate drive performance. As illustrated in Fig. (11)a), it is clear that the speed is not affected by load variation. It is also observed that the time the machine requires to reach the reference speed value (2500 rpm) with the conventional inverter (0.6s) is greater than when the machine is supplied by the five-level inverter (0.54s); the same holds true for the time needed for speed reversal.

The magnitude of pulsations in the electromagnetic torque Fig. (11)b) and stator currents Fig. (11)c) and d) show a substantial reduction for the five-level inverter compared with the two-level inverter.

The phase current quality is degraded and the torque oscillates when the level of the inverter is increased, because the supply voltage of the DSIM approximates the ideal sinusoidal voltage source when the harmonics reduce.

7. Conclusion

An enhanced NF controller has been proposed on the basis of indirect vector control of DSIM. Simulation of the IFOC and DSIM with NFC is explored using Matlab software. The behavior of the controller was tested in different cases of operating stats. A comparison was made between the proposed NFC fed by (i) conventional and (ii) five-level inverters.

The simulation results indicate that the proposed neuro-fuzzy controller is reliable and effective for speed control of the dual star induction motor in various working conditions.

References

[1] G. Singh, Multi-phase induction machine drive research—a survey, Electric Power Systems Research 61 (2) (2002) 139–147.

[2] M. Jones, E. Levi, A literature survey of state-of-the-art in multiphase ac drives, in: Proc. 37th Int. Universities Power Eng. Conf. UPEC, 2002, pp. 505–510.

[3] R. Bojoi, F. Farina, F. Profumo, A. Tenconi, Dual-three phase induction machine drives control—a survey, IEEJ Transactions on Industry Applications 126 (4) (2006) 420–429.

[4] M. Lazzari, P. Ferraris, Phase number and their related effects on the characteristics of inverter-fed induction motor drives, in: Conf. Rec. of IEEE Industry Applications Annual Meeting, IAS'83, Vol. 1, 1983, pp. 494–502.

[5] E. Levi, Recent developments in high performance variable-speed multiphase induction motor drives, in: sixth international symposium nikola tesla, 2006.

[6] S. Y. Yi, M. J. Chung, Robustness of fuzzy logic control for an uncertain dynamic system, IEEE Transactions on Fuzzy Systems 6 (2) (1998) 216–225.

[7] M. N. Uddin, T. S. Radwan, M. A. Rahman, Performances of fuzzy-logic-based indirect vector control for induction motor drive, IEEE Transactions on Industry Applications 38 (5) (2002) 1219–1225.

[8] R. Krishnan, F. C. Doran, Study of parameter sensitivity in high-performance inverter-fed induction motor drive systems, IEEE Transactions on Industry Applications (4) (1987) 623–635.

[9] R. Sadouni, A. Meroufel, Indirect rotor field-oriented control (irfoc) of a dual star induction machine (dsim) using a fuzzy controller, Acta Polytechnica Hungarica 9 (4) (2012) 177–192.

[10] S. Lekhchine, T. Bahi, Y. Soufi, Indirect rotor field oriented control based on fuzzy logic controlled double star induction machine, International Journal of Electrical Power & Energy Systems 57 (2014) 206–211.

[11] E. Merabet, H. Amimeur, F. Hamoudi, R. Abdessemed, Self–tuning fuzzy logic controller for a dual star induction machine, Journal of Electrical Engineering & Technology 6 (1) (2011) 133–138.

[12] M. Bouziane, M. Abdelkader, A neural network based speed control of a dual star induction motor, International Journal of Electrical and Computer Engineering 4 (6) (2014) 952.

[13] M. T. Wishart, R. G. Harley, Identification and control of induction machines using artificial neural networks, IEEE Transactions on Industry Applications 31 (3) (1995) 612–619.

[14] S. Lekhchine, T. Bahi, Y. Soufi, H. Merabet, Neural fuzzy speed control for six phase induction machines, Proceedings Engineering & Technology (PET) 1 (2013) 12–26.

[15] M. Nasir Uddin, M. Abido, M. Rahman, Development and implementation of a hybrid intelligent controller for interior permanent magnet synchronous motor drives, IEEE Transactions on Industry Applications 40 (1) (2004) 68–76.

[16] J.-S. Jang, Anfis: adaptive-network-based fuzzy inference system, IEEE transactions on systems, man, and cybernetics 23 (3) (1993) 665–685.

[17] J.-S. Jang, Self-learning fuzzy controllers based on temporal back-propagation, IEEE Transactions on neural networks 3 (5) (1992) 714–723.

[18] J.-S. Jang, C.-T. Sun, Neuro-fuzzy modeling and control, Proceedings of the IEEE 83 (3) (1995) 378–406.

[19] B. S. Marwa, K. M. Larbi, B. F. Mouldi, R. Habib, Modeling and analysis of double stator induction machine supplied by a multi level inverter, in: Electrotechnical Conference (MELECON), 2012 16th IEEE Mediterranean, IEEE, 2012, pp. 269–272.

[20] K. Iffouzar, S. Taraft, H. Aouzellag, K. Ghedamsi, D. Aouzellag, Behavior of a six phase induction motor fed by multilevel inverter, in: Electrical Engineering (ICEE), 2015 4th International Conference on, IEEE, 2015, pp. 1–7.

[21] K. Iffouzar, M.-F. Benkhoris, K. Ghedamsi, D. Aouzellag, Behavior analysis of a dual stars induction motor supplied by pwm multilevel inverters, REVUE ROUMAINE DES SCIENCES TECHNIQUES-SERIE ELECTROTECHNIQUE ET ENERGETIQUE 61 (2) (2016) 137–141.

[22] I. Colak, E. Kabalci, R. Bayindir, Review of multilevel voltage source inverter topologies and control schemes, Energy conversion and management 52 (2) (2011) 1114–1128.
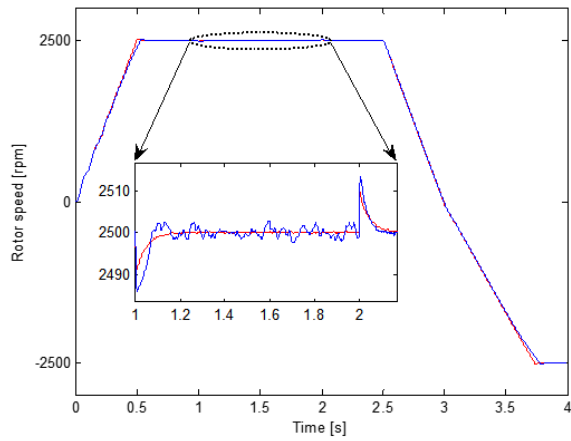
a) Rotor speed
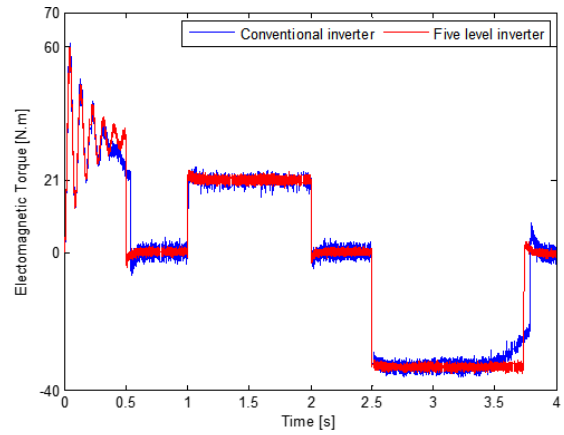
b) Electromagnetic torque
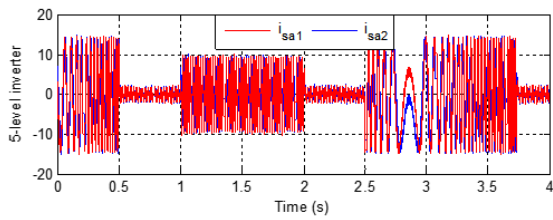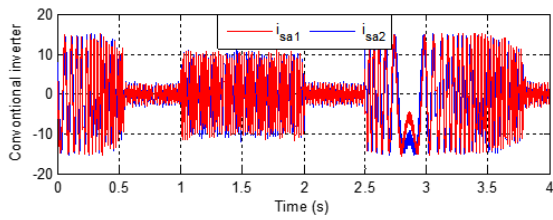
c) Stator current
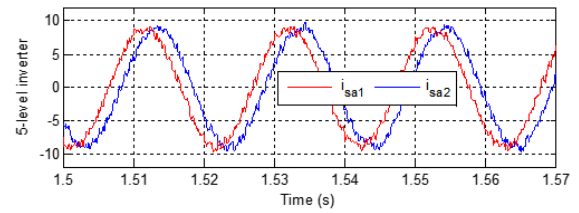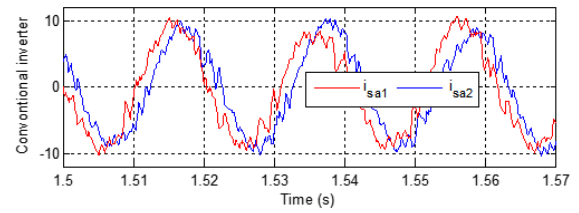
d) Phase current waveform for two inverters

Figure 11: Step changes of load torque 21N.m between 1 and 2 s and speed inversion at t=2.5 s

[23] A. Berboucha, K. Djermouni, K. Ghedamsi, D. Aouzellag, Utilisation a fuzzy controller optimized by genetic algorithm in photovoltaic pumping system, in: 7th International Conference on Electrical Engineering EEC in Batna, 2012.

[24] K. Ghedamsi, Design and realization of different strategies pwm control of the three-phase three-level inverter, Magister Memory Ecole Militaire Polytechnique.

[25] P. Thongprasri, A 5-level three-phase cascaded hybrid multilevel inverter, International Journal of Computer and Electrical Engineering 3 (6) (2011) 789.

[26] C. Elmas, O. Ustun, H. H. Sayan, A neuro-fuzzy controller for speed control of a permanent magnet synchronous motor drive, Expert Systems with Applications 34 (1) (2008) 657–664.

[27] F. Amrane, A. Chaiba, S. Mekhilef, High performances of grid-connected dfig based on direct power control with fixed switching frequency via mppt strategy using mrac and neuro-fuzzy control, Journal of Power Technologies 96 (1) (2016) 27.